Journal of Sound and Vibration 329 (2010) 2099–2113

Contents lists available at ScienceDirect

Journal of Sound and Vibration

journal homepage: www.elsevier.com/locate/jsvi

Assessment of rod behaviour theories used in spectral finite element modelling

A. Żak [a,*], M. Krawczuk [a,b]

[a] Institute of Fluid-flow Machinery, Polish Academy of Sciences, Fiszera 14, 80-952 Gdansk, Poland
[b] Gdansk University of Technology, Faculty of Electrical and Control Engineering, Narutowicza 11/12, 80-952 Gdansk, Poland

ARTICLE INFO

Article history:
Received 21 August 2009
Received in revised form
1 December 2009
Accepted 11 December 2009
Handling Editor: M.P. Cartmell
Available online 8 January 2010

ABSTRACT

In this work different theories of rods have been discussed and compared. The investigated theories are widely used in spectral finite element modelling of rod behaviour associated with propagation of symmetric longitudinal waves. These are various single, two-mode and three-mode theories including the elementary, classical Love and Mindlin–Herrmann approaches as well as new two, three and four-mode theories proposed by the authors. Dispersion curves associated with each theory, obtained by the use of Hamilton's principle, have been presented and discussed in the paper. The investigation programme carried out by the authors aimed to show major differences and similarities between the rod theories and to discuss certain numerical aspects of their application. Great attention has been paid on properties, limitations as well as difficulties associated with the use of the theories. The results obtained from a wide program on numerical tests allowed the authors to draw certain general conclusions that are valid not only in the field of the spectral finite element method but also in the field of dynamics of engineering rod structures.

1. Introduction

The phenomenon of elastic wave propagation in structural elements has been extensively studied by many researchers for last few decades. The biggest issue in accurate numerical modelling of wave propagation is structural elements comes from high frequency excitations. Such excitation regimes imply high velocities of propagating signals. Their precise representation in space and time requires very dense spacial and time discretisation making the discretisation process a key factor of any wave propagation analysis. Because of that fact many different numerical methods of modelling the wave propagation phenomenon have been reported in the literature.

Numerical methods that are currently in use to study propagation of elastic waves in structural elements can be divided into frequency domain (FD) and time domain (TD) methods. The first group of the methods covers various spectral techniques based on the frequency representation of excitation and propagating signals and is very well established in the literature. The application of the direct and inverse fast Fourier transforms (FFT, IFFT) for signal transformations between the time and frequency domains is an essential feature of these techniques.

Gopalakrishnan et al. [1] presented a methodology for development of an exact spectral Timoshenko beam element to study wave propagation in beam structures. Rizzi and Doyle [2] used a similar spectral approach to study in-plane stress waves propagating in infinite and semi-infinite planes. Danial et al. [3] investigated propagation of in-plane and

* Corresponding author.
E-mail addresses: a.zak@imp.gda.pl, azak@imp.gda.pl (A. Żak), mk@imp.gda.pl (M. Krawczuk).

0022-460X/$ - see front matter © 2009 Elsevier Ltd. All rights reserved.
doi:10.1016/j.jsv.2009.12.019

out-of-plane responses in a plate with stringers as well as in a thin-walled box beam, while Martin and Doyle [4] in their work described a method for determination of the location of an impact force using dynamic response measurements. In his work [5] Doyle presented a unified approach for various wave propagation problems in one-dimensional and two-dimensional structural elements by the use of the FFT-based spectral finite element method (SFEM). Propagation of flexural waves in a cracked isotropic plate [6] and flexural–shear coupled waves in a laminated composite beam with a crack [7] was investigated by Krawczuk et al., who employed the same methodology to solve wave propagation problems as presented by Doyle. Applying the same technique of the FFT-based spectral finite elements Mahapatra and Gopalakrishnan [8] studied propagation of axial–flexural–shear waves in thick laminated composite beams due to impact loading.

Oshima et al. [9] showed that the strip element method (SEM) formulated in the frequency domain can be applied for propagation of stress elastic waves in a beam composite fibre sensor. Similarly Liu et al. [10] investigated scattering of elastic waves by rectangular flaws in anisotropic laminated plates, while Xi et al. [11] used the same strip element technique in the frequency domain for investigation of coupled fluid–structure interaction and its influence on propagation and scattering of elastic waves in the case of a fluid-filled laminated composite cylindrical shell.

In the case of the time domain methods many different solution techniques are still in use in order to study propagation of elastic waves and are reported in the literature. The techniques that can be mentioned here include the mass spring lattice model (MSLM) and the local interaction simulation approach (LISA), the finite difference method (FDM), the method of finite elements (FEM) and boundary elements (BEM) as well as the time domain spectral finite element method (SFEM).

Simulation of ultrasonic waves in isotropic and transversely isotropic media by the use of the mass spring lattice model was carried out by Yim and Choi [12], while Chen et al. [13] studied propagation of surface acoustic waves in aluminium and copper plates excited by a laser pulse. Baek and Yim [14] employed the same technique for various wave phenomena in transversely isotropic media. Delsanto et al. [15] used the local interaction simulation approach for investigation of one-dimensional uniform waveforms propagating through a plate and in [16] presented the use of the same method in the case of two-dimensional waveforms. In a similar way Sundararaman and Adams [17] applying the local interaction simulation approach studied propagation of Lamb waves in aluminium and orthotropic plates and interactions of waves with different types of damage.

A new finite difference scheme for modelling of propagation of longitudinal and transverse waves in a heterogeneous media presented Virieux [18,19]. Various aspects associated with the stability, dissipation and convergence of different order finite difference schemes used for solving partial differential equations discussed in his work Strickwerda [20]. Harari and Turkel [21] developed fourth-order accurate finite difference methods for solving problems of propagation of harmonic acoustic waves. A review of higher order and optimised finite difference schemes used for numerical simulations of the propagation and scattering of elastic, electromagnetic and acoustic waves was given by Zingg [22]. Gosselin et al. [23] used the finite element and finite difference methods in order to solve the elastic and acoustic wave equations. Their results show that the finite element method is more efficient than the method of finite differences for the models with widely varying Poisson's ratio.

Investigation on laser induced transient Lamb waves propagating in thin plate-like and shell-like structures was carried out by Verdict et al. [24], who used the finite element method for that purpose. Koshiba et al. [25] presented a finite element based solution for scattering of the fundamental symmetric Lamb wave by a wedge-shaped internal and surface cracks in an elastic plate wave guide. A study on the effectiveness of the finite element method for modelling propagation of guided waves in annular structures was done by Moser et al. [26]. Yokoyama [27] employed the method of finite elements for investigation of one-dimensional torsional plastic waves in a thin-walled tube. Also the finite element technique was applied by Conry et al. [28], who analysed reflection and transmission of Lamb waves by embedded and surface-breaking defects in thin isotropic plates. Jeong and Ruzzene [29] studied vibration and wave propagation of cylindrical periodic grid structures by the use of the finite element method.

Zhu et al. [30] presented in their work a general boundary element approach for elastic wave propagation and scattering by cracks in laminated composite plates. A hybrid boundary element approach was employed by Clio [31] in order to investigate scattering of Lamb waves by various plate defects as well as to study the phenomena of mode conversion due to step discontinuities. Hayashi and Endoh [32] applied the same hybrid boundary element method for simulation of propagation of Lamb waves in plates. A study on the use of ultrasonic subsurface longitudinal waves for inspection of surface cracks resulting from rolling contact was performed by Lu et al. [33] who also employed the boundary element method.

The use of the spectral finite element method for various wave propagation problems starts from the work by Patera [34] who proposed a specific spectral approach based on the use of higher order Chebyshev or orthogonal Legendre polynomials combined with discretisation typical for the finite element method. Dauksher and Emery [35] analysed dispersion and accuracy of Chebyshev spectral finite element solutions in the case of one-dimensional and two-dimensional wave equations. The spectral finite element method was also employed by Komatitsch et al. [36] for investigation of elastic wave propagation in realistic geological structures in two-dimensional and three-dimensional geometries. Propagation of elastic in-plane waves in isotropic panels with damage in the form of fatigue cracks was studied by Żak et al. [37], while Ostachowicz et al. [38] demonstrated the effectiveness of the spectral finite element method for damage detection in various one-dimensional and two-dimensional structural elements. The same spectral approach was used by Kudela and Ostachowicz [39] who investigated the influence of various material parameters on propagation of transverse elastic waves corresponding to the fundamental mode of Lamb waves in a laminated composite plate.

Various one or multimode rod theories have been applied for problems related with propagation of elastic waves in rod structural elements. It should be noted that in the available literature the use of both frequency domain (FD) and time domain (TD) methods mentioned above seems to be equally reported. For example, Baz in [40], Palacz and Krawczuk in [41], Krawczuk et al. in [7] as well as Anderson in [42] applied the FFT-based spectral finite element method for their research, while at the same time Bodner and Aboudi [43], Seemann [44], Zheng et al. [45] and Kudela et al. [46] obtained their results by the use of various time domain techniques.

In this work different theories of rods have been discussed and compared. These are various single, two-mode and three-mode theories including the elementary, classical Love and Mindlin–Herrmann approaches as well as new two, three and four-mode theories proposed by the authors. Dispersion curves for each theory analysed in the paper have been presented and discussed and have been obtained by the use of Hamilton's principle. The investigation programme carried out by the authors aimed to show major differences and similarities between the rod theories and to discuss certain numerical aspects of their application. Great attention has been paid on properties, limitations as well as difficulties associated with the use of the theories. The results obtained from a wide program on numerical tests allowed the authors to draw certain general conclusions that are valid not only in the field of the spectral finite element method but also in the field of dynamics of engineering rod structures.

2. Elastic waves in rods

2.1. Theoretical background

Propagation of elastic waves in rod structural elements can be well described by the linear theory of elasticity. In the case of isotropic materials the equation of motion governing propagation of elastic waves can be expressed in a vector form as [5,47,48]):

$$\mu\nabla^2\mathbf{u}+(\lambda+2\mu)\ \text{grad}\ 0.16\text{emdiv}\,\mathbf{u}=\rho\ddot{\mathbf{u}} \tag{1}$$

where $\mathbf{u}$ is a displacement vector, λ and μ are Lamé material elastic constants, ρ denotes material density and $\ddot{\square}$ is the second time derivative.

It is most convenient to analyse this problem using the cylindrical (x,r,θ) rather than the Cartesian (x,y,z) coordinates—see Fig. 1. In the cylindrical coordinate system the components u_x, u_r and u_θ of the displacement vector $\mathbf{u}$ are certain scalar functions of the space coordinates x, r and θ as well as time t.

According to Helmholtz's theorem the field of the displacement vector $\mathbf{u}$ can be thought of as a sum of two special vector fields $\mathbf{u}_\phi$ and $\mathbf{u}_H$ such that the vector field $\mathbf{u}_\phi$ is irrotational ($\text{rot}\,\mathbf{u}_\phi=0$), while the vector field $\mathbf{u}_H$ is solenoidal ($\text{div}\,\mathbf{u}_H=0$). This is achieved by assuming that the field of the displacement vector $\mathbf{u}$ is generated by a pair of potentials, i.e. scalar potential ϕ and vector potential $\mathbf{H}=(H_x,H_r,H_\theta)$:

$$\mathbf{u}=\mathbf{u}_\phi+\mathbf{u}_H=\text{grad}\,\phi+\text{rot}\ \mathbf{H},\quad \text{div}\,\mathbf{H}=0 \tag{2}$$

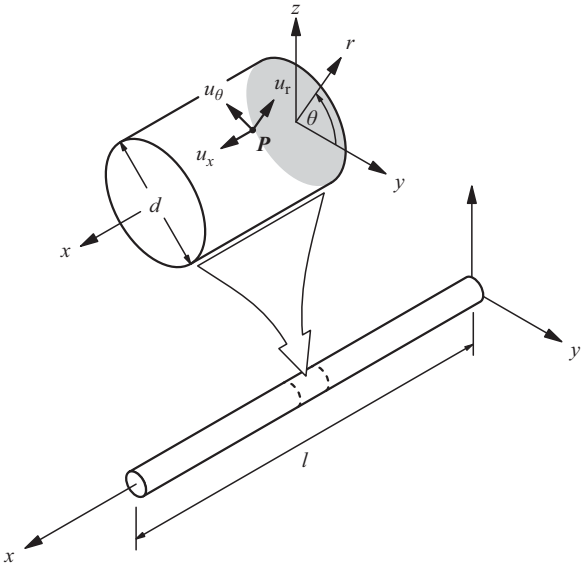

Fig. 1. Geometry of a rod structural element.

with the following notation employed:

$$\text{grad}\,\phi = \hat{\mathbf{i}}\,\frac{\partial\phi}{\partial x} + \hat{\mathbf{r}}\,\frac{\partial\phi}{\partial r} + \hat{\boldsymbol{\theta}}\,\frac{1}{r}\frac{\partial\phi}{\partial\theta}$$

$$\text{div}\,\mathbf{H} = \frac{\partial H_x}{\partial x} + \frac{1}{r}\frac{\partial(rH_r)}{\partial r} + \frac{1}{r}\frac{\partial H_\theta}{\partial\theta}$$

$$\text{rot}\,\mathbf{H} = \hat{\mathbf{i}}\,\frac{1}{r}\left[\frac{\partial(rH_\theta)}{\partial r} - \frac{\partial H_r}{\partial\theta}\right] + \hat{\mathbf{r}}\left[\frac{1}{r}\frac{\partial H_x}{\partial\theta} - \frac{\partial H_\theta}{\partial x}\right] + \hat{\boldsymbol{\theta}}\left[\frac{\partial H_r}{\partial x} - \frac{\partial H_z}{\partial r}\right]$$

$$\nabla^2 u = \frac{\partial^2 u}{\partial x^2} + \frac{\partial^2 u}{\partial r^2} + \frac{1}{r}\frac{\partial u}{\partial r} + \frac{1}{r^2}\frac{\partial^2 u}{\partial\theta^2}$$

where $\hat{\mathbf{i}}$, $\hat{\mathbf{j}}$ and $\hat{\boldsymbol{\theta}}$ are the unit vectors indicating the orientations of the x-, r- and $\theta-$axes.

Application of Helmholtz's theorem and substitution of Eq. (2) into Eq. (1) leads after some simplification and rearranging of the terms related to both potentials ϕ and $\mathbf{H}$ to

$$\text{grad}\left[(\lambda+2\mu)\nabla^2\phi - \rho\frac{\partial^2\phi}{\partial t^2}\right] + \text{rot}\left[\mu\nabla^2\mathbf{H} - \rho\frac{\partial^2\mathbf{H}}{\partial t^2}\right] = 0 \tag{3}$$

which presents in fact a set of two independent equations of motion for both potentials ϕ and $\mathbf{H}$:

$$\nabla^2\phi = \frac{1}{c_l^2}\frac{\partial^2\phi}{\partial t^2}, \quad \nabla^2\mathbf{H} = \frac{1}{c_t^2}\frac{\partial^2\mathbf{H}}{\partial t^2} \tag{4}$$

where c_l and c_t defined as follows:

$$c_l^2 = \frac{\lambda+2\mu}{\rho}, \quad c_t^2 = \frac{\mu}{\rho} \tag{5}$$

denote the velocities of longitudinal (irrotational, voluminal, dilatational or primary) and torsional (rotational, equi-voluminal, shear or secondary) waves propagating in three-dimensional unbounded isotropic media, respectively.

2.2. Pochhammer frequency equation

Investigation of elastic longitudinal waves propagating in a rod structural element can be greatly simplified by the use of the assumption about the rotational symmetry of the rod with respect to its longitudinal x axis. Due to this symmetry all displacement and strain components must be independent of the angle θ. In this case the displacement component u_θ as well as the strain components $\gamma_{x\theta}$ and $\gamma_{r\theta}$ must be equal zero, i.e. $u_\theta = \gamma_{x\theta} = \gamma_{r\theta} = 0$. Moreover, it can be shown that as a direct consequence of the symmetry the vector potential $\mathbf{H}$ must have only one non-zero component H_θ and the other two components H_x and H_r vanish, i.e. $H_x = H_r = 0$ giving $\mathbf{H} = (0, 0, H_\theta)$ [47,48]). In this way the non-zero components u_x and u_r of the displacement vector $\mathbf{u}$ within the rod can be expressed in the following way:

$$u_x = \frac{\partial\phi}{\partial x} + \frac{1}{r}\frac{\partial(rH_\theta)}{\partial r}, \quad u_r = \frac{\partial\phi}{\partial r} - \frac{\partial H_\theta}{\partial x} \tag{6}$$

which after substitution to Eq. (1) and some simplifications results in another set of two independent equations of motion expressed in terms of the scalar potentials ϕ and H_θ:

$$\nabla^2\phi = \frac{1}{c_l^2}\frac{\partial^2\phi}{\partial t^2}, \quad \nabla^2 H_\theta - \frac{H_\theta}{r^2} = \frac{1}{c_t^2}\frac{\partial^2 H_\theta}{\partial t^2} \tag{7}$$

The second equation from this set can be simplified by taking advantage of the fact that

$$\frac{\partial}{\partial r}\nabla^2\phi = \nabla^2\frac{\partial\phi}{\partial r} - \frac{1}{r^2}\frac{\partial\phi}{\partial r}$$

and by the use of the substitution $H_\theta = -\dfrac{\partial\psi}{\partial r}$ that gives:

$$\nabla^2\phi = \frac{1}{c_l^2}\frac{\partial^2\phi}{\partial t^2}, \quad \nabla^2\psi = \frac{1}{c_t^2}\frac{\partial^2\psi}{\partial t^2} \tag{8}$$

while the components u_x and u_r of the displacement vector $\mathbf{u}$ can be finally expressed as

$$u_x = \frac{\partial\phi}{\partial x} - \frac{\partial^2\psi}{\partial r^2} - \frac{1}{r}\frac{\partial\psi}{\partial r}, \quad u_r = \frac{\partial\phi}{\partial r} - \frac{\partial^2\psi}{\partial x\partial r} \tag{9}$$

The strain field within the rod can be easily evaluated based on Eqs. (9) and has the following non-zero components:

$$\varepsilon_{xx} = \frac{\partial u_x}{\partial x}, \quad \varepsilon_{rr} = \frac{\partial u_r}{\partial r}, \quad \varepsilon_{\theta\theta} = \frac{u_r}{r}, \quad \gamma_{xr} = \frac{\partial u_r}{\partial x} + \frac{\partial u_x}{\partial r} \tag{10}$$

while the stress field can be calculated from Hook's law based on the following very well-known formulas:

$$\sigma_{xx} = 2\mu\varepsilon_{xx} + \lambda(\varepsilon_{xx} + \varepsilon_{rr} + \varepsilon_{\theta\theta})$$

$$\sigma_{rr} = 2\mu\varepsilon_{rr} + \lambda(\varepsilon_{xx} + \varepsilon_{rr} + \varepsilon_{\theta\theta})$$

$$\sigma_{\theta\theta} = 2\mu\varepsilon_{\theta\theta} + \lambda(\varepsilon_{xx} + \varepsilon_{rr} + \varepsilon_{\theta\theta})$$

$$\tau_{xr} = \mu\gamma_{xr} \tag{11}$$

Harmonic waves that propagate within the rod along its longitudinal x-axis can be assumed as solutions of Eqs. (8) in a general complex form

$$\phi = \hat{\phi}(r)e^{i(kx-\omega t)}, \quad \psi = \hat{\psi}(r)e^{i(kx-\omega t)} \tag{12}$$

where $\hat{\phi}(r)$ and $\hat{\psi}(r)$ are unknown functions and k denotes the wave number while ω is the angular frequency.

Their substitution to the equations of motion (8) leads to a set of Bessel's differential equations for the functions $\hat{\phi}(r)$ and $\hat{\psi}(r)$:

$$\frac{d^2\hat{\phi}}{dr^2} + \frac{1}{r}\frac{d\hat{\phi}}{dr} + \alpha^2\hat{\phi} = 0, \quad \frac{d^2\hat{\psi}}{dr^2} + \frac{1}{r}\frac{d\hat{\psi}}{dr} + \beta^2\hat{\psi} = 0 \tag{13}$$

where

$$\alpha^2 = \frac{\omega^2}{c_l^2} - k^2, \quad \beta^2 = \frac{\omega^2}{c_t^2} - k^2$$

that has solutions in the form of Bessel functions of the first $J_0(\alpha r)$ and $J_0(\beta r)$ as well as Bessel functions of the second $Y_0(\alpha r)$ and $Y_0(\beta r)$ kind. Because the Bessel functions of the second kind exhibit singular behaviour at their origin at $r = 0$ this branch of the solution is discarded leading to the following form of the solution of the problem under investigation:

$$\hat{\phi}(r) = AJ_0(\alpha r), \quad \hat{\psi}(r) = BJ_0(\beta r) \tag{14}$$

where A and B are certain constants.

Taking into account the general form of the solutions from Eqs. (12) it can be finally written that:

$$\phi = AJ_0(\alpha r)e^{i(kx-\omega t)}, \quad \psi = BJ_0(\beta r)e^{i(kx-\omega t)} \tag{15}$$

Propagation of elastic longitudinal waves in the rod requires the fulfilment of zero-traction boundary conditions on the rod outer surface that accompany the set of the equations of motion given by (8):

$$\sigma_{rr}(x, r) = \tau_{xr}(x, r) = 0 \quad \text{for } 0 \le x \le l, \quad r = a = \frac{d}{2} \tag{16}$$

where l is the length and d is the diameter of the rod.

The zero-traction boundary conditions for the stress components σ_{rr} and τ_{xr}, after substitution of Eqs. (15) to Eqs. (10) and by the subsequent use of the formulas from Eqs. (11) and some simplification, form a set of two homogeneous equations expressed in terms of the two solutions from Eqs. (15).

The given set of equations has a non-trivial solution only then when its determinant vanishes. In the case under consideration this condition leads directly to a certain nonlinear equation known in the literature as the Pochhammer frequency equation for longitudinal modes propagating in rods and which links together the angular frequency ω and the wave number k. The Pochhammer frequency equation has the following form:

$$\frac{2\alpha}{a}(\beta^2 + k^2)J_1(\alpha a)J_1(\beta a) - (\beta^2 - k^2)^2 J_0(\alpha a)J_1(\beta a) + -4k^2\alpha\beta J_1(\alpha a)J_0(\beta a) = 0 \tag{17}$$

It is interesting to note that this equation was originally introduced by a Prussian mathematician Pochhammer [49] in 1876 who studied vibration behaviour of circular cylinders. This equation was also studied by many other researches [50–54] and due its complexity the roots of the equation remained unknown for many years.

2.3. Solution of the Pochhammer frequency equation

In the current case the Pochhammer frequency equation was solved by the use of an original and dedicated program written by the authors in *Matlab* environment [55]. The values of the velocities of longitudinal c_l and torsional c_t waves propagating in the rod were calculated assuming the rod made out of aluminium with Young's modulus $E = 72.7$ GPa, Poisson's ratio $\nu = 0.33$ and material density $\rho = 2700\,\text{kg/m}^3$ and of the diameter $d = 0.01$ m. The values of the characteristic velocities were $c_l = 6.3$ km/s and $c_t = 3.2$ km/s, respectively.

As a calculation domain the frequency range f from 0.1 Hz up to 2.0 MHz and the phase velocity range c_P from 2 km/s up to 50 km/s was chosen. The roots of the Pochhammer frequency equation were sought at nodes of a regular grid of 400×2000 nodes at the assumed accuracy level $\delta \le 0.001$percent.

The solution was based on the use of a conjugate bisection method developed by the authors [56]. In the first step the roots were found as a function of the phase velocity $c_p = \omega/k$ for given values of the frequency $f = \omega/2\pi$ treated as a parameter in Eq. (17). In the second step the phase velocity c_p was assumed to be a parameter and the roots were found as a function of the frequency f. In this way the second step of calculations improved the solutions obtained from the first step for those regions of analysis where changes in the phase velocity c_p as a function of the frequency f were of a very high magnitude.

The results obtained for changes in the phase velocity c_p as a function of a frequency parameter defined as fd are shown in Fig. 2, while Fig. 3 presents changes in the group velocity c_g as a function of the same frequency parameter fd. The values of the group velocity $c_g = \mathrm{d}\omega/\mathrm{d}k$ were also obtained numerically by differentiation of the wave number curves $k = k(\omega)$ with respect to the angular frequency ω.

As it can be seen from Fig. 4 the phase velocity curve $c_p = c_p(fd)$ for the second propagation mode exhibits some very unusual behaviour just above the cut-off frequency for this mode and between points A, B and C. It can be seen that the

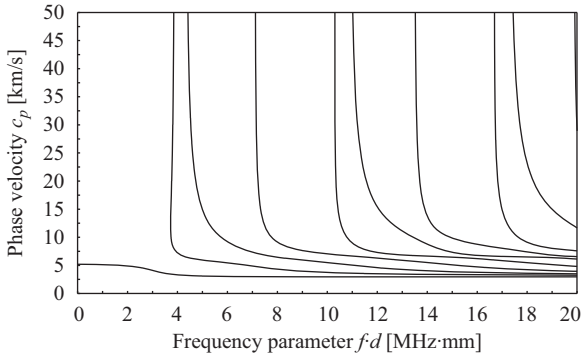

Fig. 2. Phase velocity c_p dispersion curves for an aluminium rod ($c_l = 6.3$ km/s, $c_t = 3.2$ km/s).

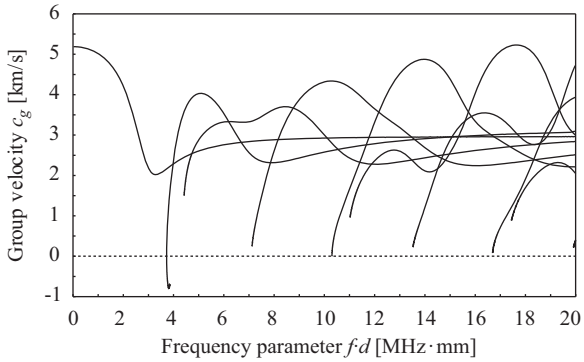

Fig. 3. Group velocity c_g dispersion curves for an aluminium rod ($c_l = 6.3$ km/s, $c_t = 3.2$ km/s).

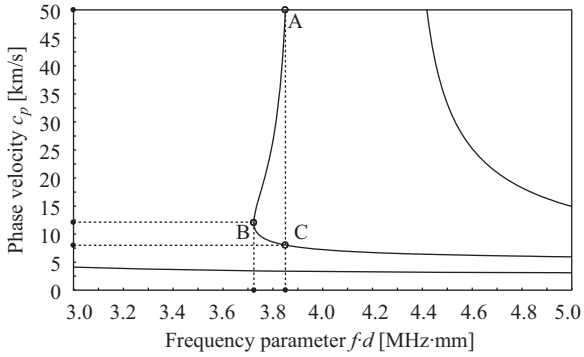

Fig. 4. Magnification of the behaviour of the second mode of the phase velocity c_p dispersion curve for an aluminium rod ($c_l = 6.3$ km/s, $c_t = 3.2$ km/s).

opposite signs of the phase c_p and the group c_g velocities between points A and B suggests a possibility that the direction of energy transmission in the rod can be opposite to the direction of wave motion. Such a phenomenon of the so-called *backward wave propagation* was studied and reported in the literature in the past by many researches [57–60] and still is a subject of research especially in the case of electromagnetic waves.

In the range of the frequency parameter fd starting from the cut-off frequency of 3.72 MHz mm (point B) up to 3.85 MHz mm (points A and C) the phase velocity curve c_p is double valued, which indicates two different zones for the values of the group velocity c_g. The first branch of the phase velocity curve $c_p = c_p(fd)$ between point A and B is a high phase velocity region, where the phase velocity c_p and the group velocity c_g have opposite signs. The second branch between points B and C is a low phase velocity region, where the phase velocity c_p and the group velocity c_g have the same signs.

3. Rod theories

3.1. General considerations

The rod theories that are widely exploited in the literature and related to propagation of elastic waves in rod structural elements can be classified and grouped as one-mode, two-mode, three-mode and higher mode theories. A number of theories based on different displacement fields can be obtained based on the careful analysis of a general three-dimensional displacement field of a rod structural element. Appropriate Maclaurin series expansion helps to reduce the number of unknown variables to a desired and necessary number. It should be emphasised that the reduced number of the unknown variables simplifies not only the complexity of the displacement fields but also reduces the number of wave modes than are allowed by the theories limiting their application range.

Using the same cylindrical coordinates (x, r, θ) expansion into a Maclaurin series, for example, of the component u_x of the rod displacement field about $r = 0$ leads to the following equation:

$$u_x(x, r, \theta) = u_x(x, 0, \theta) + \sum_{n=1}^{\infty} \frac{\partial^n u_x(x, 0, \theta)}{\partial r^n} \frac{r^n}{n!} \tag{18}$$

It should be mentioned here in the case the component u_x the terms that are proportional to the odd values of n are related with antisymmetric behaviour and propagation of bending waves, while the terms proportional to the even values of n are related to symmetric behaviour and propagation of longitudinal waves. The same expansion into a Maclaurin series repeated for the component u_r leads to opposite conclusions [5,47,48].

A number of terms kept in the series given by (18) depends on the investigated phenomena and is directly related with the total number of degrees of freedom of any finite element approximation based on the series expansion. The expansion of the component u_x at $n = 2$ gives the Maclaurin series of the following form:

$$u_x(x, r, \theta) = u_x(x, 0, \theta) + \frac{\partial u_x(x, 0, \theta)}{\partial r} r + \frac{1}{2} \frac{\partial^2 u_x(x, 0, \theta)}{\partial r^2} : r^2 + E(r^3) \tag{19}$$

where $E(r^3)$ represents the truncation error of the expansion proportional to r^3. At this point a step towards a finite element approximation can be made and then Eq. (19) can be rewritten as

$$u_x(x, r, \theta) = \tilde{u}_x(x, \theta) + \tilde{\phi}_0(x, \theta) r + \tilde{\phi}_1(x, \theta) r^2 \tag{20}$$

where now $\tilde{u}_x(x, \theta)$, $\tilde{\phi}_0(x, \theta)$ and $\tilde{\phi}_1(x, \theta)$ may be thought of as denoting degrees of freedom of a rod finite element associated with a Maclaurin expansion of the component u_x of the rod displacement field.

It is obvious that due to the truncation of the series (19) the obtained formula (20) is not exact and it represents the three-dimensional displacement field of a rod structural element in an approximated sense. However, it should be emphasised that effective solutions of most of the engineering problems involving static or dynamic problems require finite elements that employ only the first two or three terms of an appropriate Maclaurin series. In the case considered above it can be noted immediately that

$$\tilde{u}_x(x, \theta) = u_x(x, 0, \theta)$$

$$\tilde{\phi}_0(x, \theta) = \frac{\partial u_x(x, 0, \theta)}{\partial r}$$

$$\tilde{\phi}_1(x, \theta) = \frac{1}{2} \frac{\partial^2 u_x(x, 0, \theta)}{\partial r^2} \tag{21}$$

Contrary, a great majority of problems involving propagation of elastic waves in one or two-dimensional structural elements require much more accurate representation of the three-dimensional behaviour of a solid element. This is directly related with modelling of different modes of elastic waves propagating within such three-dimensional solid structures.

The wave propagation phenomena is related with a coupled interaction of shear and extensional waves propagating within a structure with structural lateral boundaries. As a result of this coupled interaction propagation of various modes

of elastic waves can be observed. Appropriate representation of these modes in a broad range of wave propagation frequencies requires a greater number of terms of a Maclaurin series in order to capture the complexity of the interaction phenomena. For that reason special types of new finite elements are developed that are known in the literature as *spectral finite elements*.

3.2. Displacement fields

As mentioned before propagation of elastic longitudinal waves in rod structural elements is associated with rod symmetric behaviour. Therefore based on Eq. (18) and the following considerations the general form of the displacement field of a one-dimensional rod spectral finite element for analysis of propagation of elastic longitudinal waves can be written in the following way:

$$u_x(x,r)=\tilde{u}_x(x)+\tilde{\phi}_2(x)r^2+\tilde{\phi}_4(x)r^4$$

$$u_r(x,r)=\tilde{\psi}_1(x)r+\tilde{\psi}_3(x)r^3+\tilde{\psi}_5(x)r^5 \tag{22}$$

where only six terms of the Maclaurin series expansions of the displacement components u_x and u_r are used. It can be reminded here that due to the rotational symmetry of the rod with respect to its longitudinal x all displacement and strain components must be independent of the angle θ.

The function $\tilde{u}_x(x)$ as well as the functions $\tilde{\phi}_i(x)$ $(i=2,4)$ and $\tilde{\psi}_j(x)$ $(j=1,3,5)$ defined in Eqs. (22) represent the independent nodal variables or degrees of freedom of the rod spectral finite element. It can be seen that in the current formulation the rod element has as many as 6 degrees of freedom in a single node. This number of independent nodal variables may be reduced, however, by taking into account the zero traction condition (16) rewritten here:

$$\sigma_{rr}(x,r)=\tau_{xr}(x,r)=0 \quad \text{for } 0\le x\le l, \quad r=a=\frac{d}{2} \tag{23}$$

where now l denotes the length and d is the diameter of the rod spectral finite element—see Fig. 1.

Based on the form of the displacement field given by Eqs. (22) the displacement fields for various one-mode, two-mode and other multimode rod theories can be built. Additionally the use of Eqs. (23) representing the zero traction conditions on the lateral boundaries of the rod element allows one to enrich the displacement fields by some additional higher order terms. However, in most cases the resulting set of two differential equations is very complicated and cannot be solved analytically.

This problem can be avoided by a simple mathematical substitution thanks to which the zeroth-order terms for both displacement components u_x and u_r can be represented as sums of all order terms. In the current case this condition takes the following form—for clarity and simplicity of the presentation the arguments x, r will be omitted hereinafter:

$$\overline{u}_x=\tilde{u}_x-\phi_2-\phi_4, \quad \phi_2=-\tilde{\phi}_2a^2, \quad \phi_4=-\tilde{\phi}_4a^4$$

$$\psi_1=\tilde{\psi}_1-\psi_3-\psi_5, \quad \psi_3=-\tilde{\phi}_3a^2, \quad \psi_5=-\tilde{\psi}_5a^4 \tag{24}$$

Taking into account Eqs. (24) a new form of the displacement field of a one-dimensional rod spectral finite element for analysis of propagation of elastic longitudinal waves can be expressed as:

$$u_x=\overline{u}_x+\phi_2\left[1-\left(\frac{r}{a}\right)^2\right]+\phi_4\left[1-\left(\frac{r}{a}\right)^4\right]$$

$$u_r=\psi_1r+\psi_3\left[1-\left(\frac{r}{a}\right)^2\right]r+\psi_5\left[1-\left(\frac{r}{a}\right)^4\right]r \tag{25}$$

Particular theories of rod symmetric behaviour known from the literature can be easily obtained based on Eqs. (23) and (25). Different rod theories can be associated with different forms of the functions ϕ_i $(i=2,4)$ and ψ_j $(j=1,3,5)$. It is very convenient to present them in the following manner:

- elementary single-mode theory:

$$\phi_2=\phi_4=\psi_1=\psi_3=\psi_5=0 \tag{26}$$

- single-mode Love theory [51]:

$$\phi_2=\phi_4=\psi_1=\psi_3=\psi_5=0 \tag{27}$$

with an additional equation resulting from the assumption about the coupling between the longitudinal velocity $\dot{u}_x$ and the transverse velocity $\dot{u}_r$ through Poisson's ratio effect $\dot{\varepsilon}_{rr}=-\nu\dot{\varepsilon}_{xx}$ influencing rod kinetic energy:

$$\dot{u}_r=-\nu r\frac{\mathrm{d}\dot{u}_x}{\mathrm{d}x}$$

- two-mode Mindlin–Herrmann theory [61]:

$$\phi_2 = \phi_4 = \psi_3 = \psi_5 = 0 \tag{28}$$

- higher order two-mode theory (authors):

$$\phi_2 = \frac{a^2}{2}\frac{\mathrm{d}\psi_1}{\mathrm{d}x}, \quad \psi_3 = \frac{\mu+\lambda}{2\mu+\lambda}\psi_1 + \frac{\lambda}{2(2\mu+\lambda)}\frac{d\overline{u}_x}{dx}$$

$$\phi_4 = \psi_5 = 0 \tag{29}$$

- three-mode theory [5]:

$$\phi_4 = \psi_3 = \psi_5 = 0 \tag{30}$$

- higher order three-mode theory (authors):

$$\phi_4 = \frac{a^2}{4}\left(\frac{\mathrm{d}\psi_1}{\mathrm{d}x} - \frac{1}{2}\phi_2\right), \quad \psi_3 = \frac{\mu+\lambda}{2\mu+\lambda}\psi_1 + \frac{\lambda}{2(2\mu+\lambda)}\frac{\mathrm{d}\overline{u}_x}{\mathrm{d}x}$$

$$\psi_5 = 0 \tag{31}$$

- four-mode theory [42]:

$$\phi_4 = \psi_5 = 0 \tag{32}$$

- higher order four-mode theory (authors):

$$\phi_4 = \frac{a^2}{4}\left(\frac{\mathrm{d}\psi_1}{\mathrm{d}x} - \frac{1}{2}\phi_2\right)$$

$$\psi_5 = \frac{\mu+\lambda}{2(2\mu+\lambda)}\psi_1 - \frac{1}{2}\psi_3 + \frac{\lambda}{4(2\mu+\lambda)}\frac{\mathrm{d}\overline{u}_x}{\mathrm{d}x} \tag{33}$$

It should be stressed out that the physical meaning of the higher order terms ϕ_i $(i=2,4)$ and ψ_j $(j=3,5)$ must always be connected together with the form of a particular displacement field under consideration and results from certain mathematical manipulations that influence it. In the current approach these terms express higher order corrections to the initially assumed distributions of the longitudinal and transverse displacement components.

3.3. Dispersion curves

Dispersion curves for a particular rod theory carry very important information about certain frequency characteristics of the theory, but most of all the range of its application and agreement with the Pochhammer analytical solution. In the case of the displacement fields presented in the previous section and associated with the different rod theories the dispersion curves can be evaluated based on a very simple procedure.

In a first step it is necessary to determine equations of motion associated with the rod theory under consideration and this can be easily achieved by the use of Hamilton's principle. Based on the given displacement field the virtual work W related to deformation and motion of a rod structural element may be expressed in terms of its strain energy U, kinetic energy T as well as the work of some external forces F. Application of Hamilton's principle at this point leads to a set of equations of motion that are derived for each component of the displacement field, as presented by Doyle in [5].

In the following step propagation of harmonic waves within a rod structural element is assumed. This helps to transform the equations of motion from a set of partial differential equations, defined in the time domain for each displacement component, to a set of linear homogeneous equations defined in the frequency domain but for the amplitudes of each displacement component. This system can be solved only then when its determinant vanishes, which leads directly to a characteristic polynomial equation. The roots of the characteristic polynomial equation define dispersion relations between particular modes of harmonic waves that can propagate within the rod, the wave number k and the angular frequency ω of these waves.

The dispersion curves for each rod theory discussed in this paper were obtained by the use of the *Mathematica* package [62] that was applied for all required analytical manipulations, while for necessary numerical calculations related with evaluation of the dispersion curves the authors employed the *Matlab* package [55].

The above-mentioned procedure is discussed here in more details for the two-mode Mindlin–Herrmann theory of rod behaviour from the previous section of the paper. In the case of the two-mode Mindlin–Herrmann theory taking into account Eqs. (25) as well as the relations given by Eqs. (28) leads to the displacement field in the following simple form:

$$u_x = \overline{u}_x$$

$$u_r = \psi_1 r \tag{34}$$

for which the strain energy U and the kinetic energy T can be evaluated from

$$T=\frac{1}{2}\iiint_V \rho\tilde{T}\,\mathrm{d}V,\quad U=\frac{1}{2}\iiint_V \tilde{U}\,\mathrm{d}V \tag{35}$$

where ρ is the rod material density and V denotes the volume of the rod:

$$\tilde{T}=\left(\frac{\partial\overline{u}_x}{\partial t}\right)^2+r^2\left(\frac{\partial\psi_1}{\partial t}\right)^2$$

$$\tilde{U}=(\lambda+2\mu)\left(\frac{\partial\overline{u}_x}{\partial x}\right)^2+r^2\left(\frac{\partial\psi_1}{\partial x}\right)^2+4\lambda\frac{\partial\overline{u}_x}{\partial x}\psi_1+4(\lambda+\mu)\psi_1^2 \tag{36}$$

The application of Hamilton's principle and integration by parts of Eqs. (35) leads to equations of motion associated with the two-mode Mindlin–Herrman theory of rod behaviour. These equations can be written as a set of two following partial differential equations:

$$\rho\frac{\partial^2\overline{u}_x}{\partial t^2}=(\lambda+2\mu)\frac{\partial^2\overline{u}_x}{\partial x^2}+2\lambda\frac{\partial\psi_1}{\partial x}$$

$$a^2\rho\frac{\partial^2\psi_1}{\partial t^2}=a^2\mu\frac{\partial^2\psi_1}{\partial x^2}-4\lambda\frac{\partial\overline{u}_x}{\partial x}-8(\lambda+\mu)\psi_1 \tag{37}$$

Eqs. (37) describe motion of rod structural elements according to the two-mode Mindlin–Herrmann theory and couple spacial changes in the displacement components $\overline{u}_x$ and ψ_1 with changes in time t. However, in order to obtain the dispersion curves, which express changes in the phase c_p and group c_g velocities as a function of the angular frequency ω or the frequency $f=\omega/2\pi$, for the two modes of elastic longitudinal waves associated with the Mindlin–Herrmann theory of rods, the equations of motion (37) must be transformed from the time domain into the frequency domain. For that purpose it is convenient to assume that the displacement components $\overline{u}_x$ and ψ_1 can be expressed as solutions of the equations of motion:

$$\overline{u}_x=\langle\overline{u}_x\rangle\exp[-\mathrm{i}(kx-\omega t)]$$

$$\psi_1=\langle\psi_1\rangle\exp[-\mathrm{i}(kx-\omega t)] \tag{38}$$

where $i=\sqrt{-1}$ is the imaginary unit and ω and k denote the angular frequency and the wave number, respectively.

A system of two linear homogeneous equations can be obtained for each harmonic amplitude component $\langle\overline{u}_x\rangle$ and $\langle\psi_1\rangle$ by simple substitution of Eq. (38) into Eq. (37) and some simplifications:

$$\{\rho\omega^2-k^2(\lambda+2\mu)\}\langle\overline{u}_x\rangle-\{2\lambda ik\}\langle\psi_1\rangle=0$$

$$\{4\lambda ik\}\langle\overline{u}_x\rangle-\{8\lambda+(8+a^2k^2)\mu-a^2\rho\omega^2\}\langle\psi_1\rangle=0 \tag{39}$$

This system has a non-trivial solution only then when its determinant vanishes, which leads to a characteristic polynomial equation associated with the current problem:

$$\mu(\lambda+2\mu)a^2k^4+(a^2\rho\omega^2-8(\lambda+\mu))\rho\omega^2+(8\mu(3\lambda+2\mu)-(\lambda+3\mu)a^2\rho\omega^2)k^2=0 \tag{40}$$

being the fourth-order polynomial equation with respect to the wave number k and being a function of the angular frequency ω. This characteristic polynomial equation has two real and positive roots that are related with the two modes of elastic longitudinal waves that can propagate within a rod structural element and allowed by the two-mode Mindlin–Herrmann theory. These roots can be calculated numerically for any chosen value of the angular frequency ω and thanks to the obtained relation $k=k(\omega)$ the phase velocity $c_p=\omega/k$ as well as the group velocity $c_g=\mathrm{d}\omega/\mathrm{d}k$ can be easily calculated and plotted, as presented in Fig. 7.

Exactly the same procedure was used in order to calculate the remaining dispersion curves associated with the other rod theories presented and discussed in the previous section of the paper.

3.4. Comparison of rod theories

It can be expected that various rod theories known from the literature and employed to study propagation of elastic longitudinal waves in rod structural elements agree with the Pochhammer analytical solution within a limited frequency range. Depending on the rod theory this frequency range is different and may cover propagation of one, two or even more wave modes. For the rod theories discussed in the previous section of this paper this is very well seen in Figs. 5–12, which present dispersion curves for the ratio of the group velocity c_g to the phase velocity c_p.

It is very well seen from Figs. 5 to 12 that the agreement between the Pochhammer analytical solution and particular rod theories increases with the number of additional higher modes used by the theories. It should be mentioned that for the four-mode theories the dispersion curve for the fourth wave mode is not observable and lies beyond the investigated frequency range.

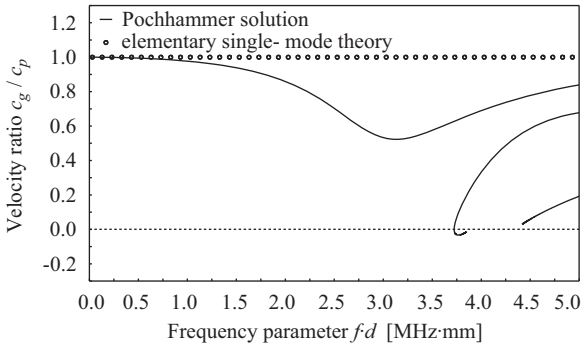

Fig. 5. Dispersion curve for the velocity ratio c_g/c_p for the elementary single-mode theory of rods ($c_l = 6.3$ km/s, $c_t = 3.2$ km/s).

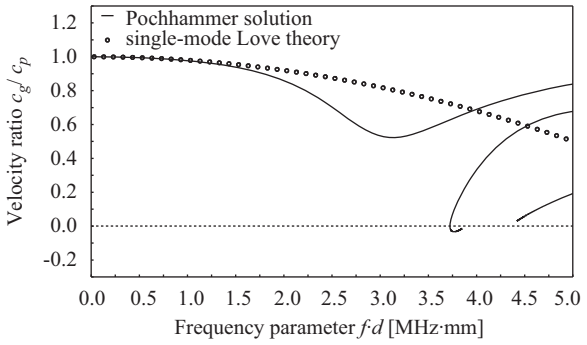

Fig. 6. Dispersion curve for the velocity ratio c_g/c_p for the single-mode Love theory of rods ($c_l = 6.3$ km/s, $c_t = 3.2$ km/s).

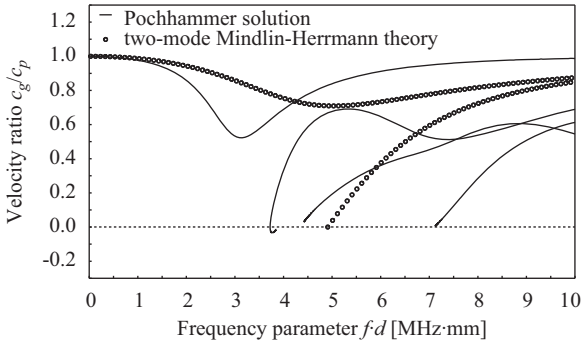

Fig. 7. Dispersion curve for the velocity ratio c_g/c_p for the two-mode Mindlin–Herrmann theory of rods ($c_l = 6.3$ km/s, $c_t = 3.2$ km/s).

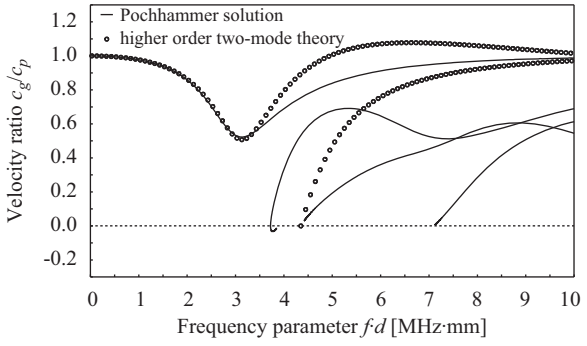

Fig. 8. Dispersion curve for the velocity ratio c_g/c_p for the higher order two-mode theory of rods ($c_l = 6.3$ km/s, $c_t = 3.2$ km/s).

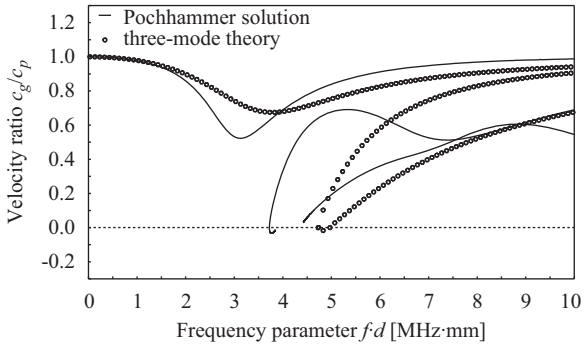

Fig. 9. Dispersion curve for the velocity ratio c_g/c_p for the three-mode theory of rods ($c_l = 6.3$ km/s, $c_t = 3.2$ km/s).

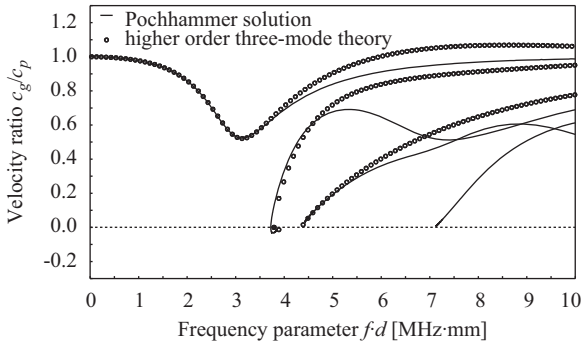

Fig. 10. Dispersion curve for the velocity ratio c_g/c_p for the higher order three-mode theory of rods ($c_l = 6.3$ km/s, $c_t = 3.2$ km/s).

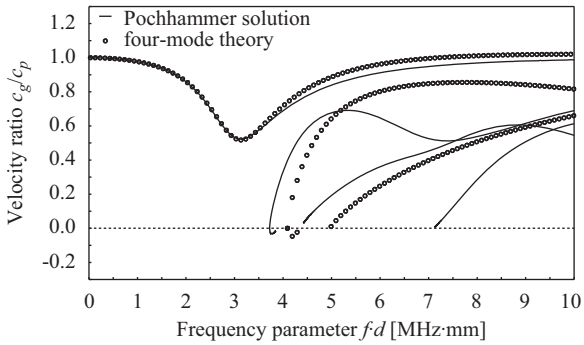

Fig. 11. Dispersion curve for the velocity ratio c_g/c_p for the four-mode theory of rods ($c_l = 6.3$ km/s, $c_t = 3.2$ km/s).

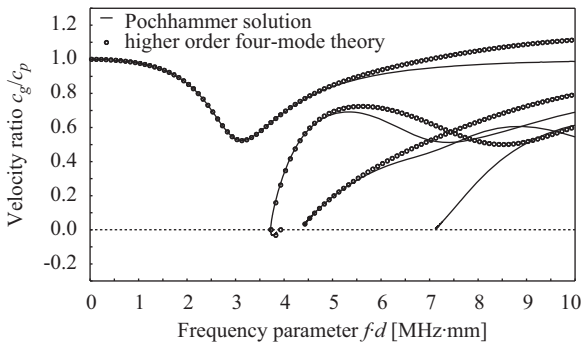

Fig. 12. Dispersion curve for the velocity ratio c_g/c_p for the higher order four-mode theory of rods ($c_l = 6.3$ km/s, $c_t = 3.2$ km/s).

It is interesting to note that the additional modes have the greatest influence on the behaviour of the dispersion curves related with propagation of the fundamental wave mode and within the frequency range up to the first cut-off frequency. It can be explained by the fact that the behaviour of the fundamental mode within this frequency range is described by all degrees of freedom used by different rod theories, while above it the same number of degrees of freedom is available to describe the behaviour of not only the fundamental but also all higher wave modes.

It should be noticed that for all higher order rod theories investigated (Love in Fig. 6, two-mode in Fig. 8, three-mode in Fig. 10, four-mode in Fig. 12) the agreement between the dispersion curves from the Pochhammer analytical solution and the dispersion curves obtained from the rod theories is much better than in the case of ordinary higher-mode theories (elementary in Fig. 5, two-mode Mindlin–Herrmann in Fig. 7, three-mode in Fig. 9 and four-mode in Fig. 11).

The applicability of the higher order three and four-mode rod theories extends also to the frequency range that covers the first and the second cut-off frequency, respectively. The reason for that becomes obvious if one refers back to the zero-traction boundary conditions expressed by Eqs. (8). The fulfilment of these conditions allows one to enrich the displacement fields of higher order theories by two higher order terms making the obtained solution closer to the Pochhammer analytical solution. These higher order terms may be thought of as being equivalent to two additional but dependent degrees of freedom. However, the zero-traction boundary conditions are not fulfilled for ordinary higher-mode theories, although the theories make use of similar higher order terms in their displacement fields. The influence of the higher order terms is especially well illustrated in the case of the higher order two-mode theory presented in Fig. 8 and the three and four-mode theories presented in Fig. 9 and Fig. 11 in the frequency range up to the first cut-off frequency.

It should be understood that the usefulness of a particular rod theory to study various wave propagation problems in rod structural elements depends most of all on the frequency range of interest. For that reason even the lower-mode theories (elementary or Love) can be successfully applied in all such cases, where the bandwidth of excitation is narrow and the excitation frequencies are low. At the same time the higher-mode theories or higher order theories can be used for much wider bandwidths of high frequency excitations. It can be noticed from Figs. 5 to 12, however, that even higher order and higher-mode theories discussed in this paper are applicable for the excitation frequencies slightly above the first cut-off frequency. For the higher order four-mode theory this frequency range covers also the second cut-off frequency and in the case of the aluminium rod under investigation can be estimated as 5.0 MHz mm.

Changes in the relative error δ are illustrated in Fig. 13 as a function of the frequency parameter fd for each rod theory discussed in the paper calculated against the Pochhammer analytical solution for the fundamental propagation mode. This relative error was evaluated based on the appropriate ratios of the group velocity c_g and the phase velocity c_p as

$$\delta = \left(\frac{c_1}{c_2} - 1\right) \times 100\% \tag{41}$$

where c_1 denotes the velocity ratio c_g/c_p obtained by the use of a selected rod theory, while c_2 refers to the velocity ratio c_g/c_p obtained from the Pochhammer analytical solution.

According to the results presented in Fig. 13 it can be found out that in the case of the aluminium rod under consideration the elementary and Love theories of rod behaviour can be practically used up to 1.4 and 1.9 MHz mm, respectively. This bandwidth for applications of the theories ensures that the relative error δ, between the results based on the theories and the Pochhammer analytical solution stays below 5 percent. In a similar manner it can be found out that for the two-mode Mindlin–Herrmann theory, the higher order two-mode and the three-mode theories the appropriate values of the frequency parameters are 1.7, 3.5 and 2.0 MHz mm. It is worth to point out that the relative error δ for these rod theories increases greatly with an increase in the frequency parameter fd and has its maximum value at the first cut-off frequency denoted as point B in Fig. 13. After this point the relative error δ decreases.

For the four-mode as well as higher order three and four-mode rod theories the relative error δ never reaches the value of 5 percent within the frequency range assumed. The greatest relative error δ equal to 4 percent is associated with the use

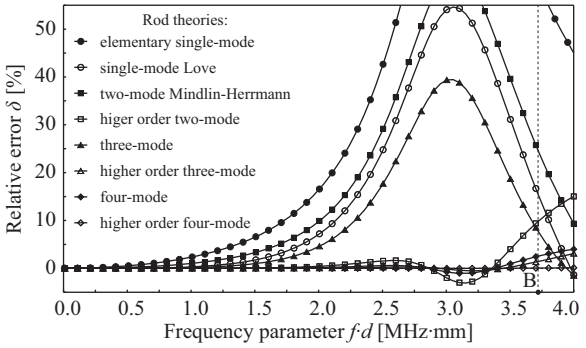

Fig. 13. Relative errors for various rod theories measured against Pochhammer analytical solution for the first propagation mode ($c_l = 6.3$ km/s, $c_t = 3.2$ km/s).

of the four-mode theory, while in the case of the higher order three and four-mode theories the values of the relative error δ are around 3 percent and 0.1 percent, respectively.

In general, it can be said that within the investigated frequency range all higher order theories give better results than equivalent ordinary theories, therefore in order to ensure low levels of modelling errors it should be recommended to employ rather higher order lower-mode theories of rod behaviour than ordinary higher-mode theories.

4. Conclusions

This paper presents results of analytical and numerical investigation and comparison of different theories that are widely used in spectral finite element modelling of rod behaviour associated with propagation of symmetric longitudinal waves. This analysis comprised various single, two-mode and three-mode theories including the elementary, classical Love and Mindlin–Herrmann approaches known from the literature as well as new two, three and four-mode theories proposed by the authors. Appropriate dispersion curves associated with each theory, obtained by the use of Hamilton's principle, have been presented and discussed in the paper.

As expected the investigated rod theories employed to study propagation of elastic longitudinal waves in rod structural elements show a good agreement with the Pochhammer analytical solution within different and limited frequency ranges. Depending on the theory this frequency range varies and may cover propagation of one, two or even more wave modes. The investigation programme carried out by the authors showed major differences and similarities between the theories and great attention has been paid on properties, limitations as well as difficulties associated with the use of the theories.

References

[1] S. Gopalakrishnan, M. Martin, J.F. Doyle, A matrix methodology for spectral analysis of wave propagation in multiple connected Timoshenko beams, *Journal of Sound and Vibration* 158 (1992) 11–24.
[2] S.A. Rizzi, J.F. Doyle, Spectral analysis of wave motion in plane solids with boundaries, *Journal of Vibration, Acoustics, Stress, and Reliability in Design* 114 (1992) 133–140.
[3] A.N. Danial, J.F. Doyle, S.A. Rizzi, Dynamic analysis of folded plate structures, *Journal of Vibration and Acoustics, Transactions of the ASME* 118 (1996) 591–598.
[4] M.T. Martin, J.F. Doyle, Impact force location in frame structures, *International Journal of Impact Engineering* 18 (1996) 79–97.
[5] J.F. Doyle, *Wave Propagation in Structures*, Springer New York Inc, New York, 1997.
[6] M. Krawczuk, M. Palacz, W. Ostachowicz, Spectral plate element for crack detection with the use of propagating waves, *Materials Science Forum* 440–441 (2003) 187–194.
[7] M. Krawczuk, M. Palacz, W. Ostachowicz, Flexural–shear wave propagation in cracked composite beam, *Science and Engineering of Composite Materials* 11 (2004) 55–67.
[8] R.D. Mahapatra, S. Gopalakrishnan, A spectral finite element model for analysis of axial–flexural–shear coupled wave propagation in laminated composite beams, *Computers and Structures* 59 (2003) 67–88.
[9] T. Oshima, R.D. Kriz, S.G. Nomachi, Visual simulation of stress wave propagation in fiber sensor with interphase layer in composite laminate, *American Society of Mechanical Engineers, Aerospace Division* 35 (1993) 401–406.
[10] G.R. Liu, K.Y. Lam, H.M. Shang, Scattering of waves by flaws in anisotropic laminated plates, *Composites Part B: Engineering* 27 (1996) 431–437.
[11] Z.C. Xi, G.R. Liu, K.Y. Lam, H.M. Shang, A strip-element method for analyzing wave scattering by a crack in a fluid-filled composite cylindrical shell, *Composites Science and Technology* 60 (2000) 1985–1996.
[12] H. Yim, Y. Choi, Simulation of ultrasonic waves in various types of elastic media using the mass spring lattice model, *Materials Evaluation* 58 (2000) 889–896.
[13] T. Chen, S. Yuan, J. Lu, X.W. Ni, Numerical simulation of the surface acoustic wave propagated on the plate surface by mass spring lattice model, *Journal of Nanjing Institute of Posts and Telecommunications* 25 (2005) 75–78.
[14] E. Baek, H. Yim, Use of a mass–spring lattice model for simulating ultrasonic waves in an anisotropic elastic solid, *AIP Conference Proceedings* 820 I (2006) 41–48.
[15] P.P. Delsanto, T. Whitecomb, H.H. Chaskelis, R.B. Mignogna, Connection machine simulation of ultrasonic wave propagation in materials. I: the one-dimensional case, *Wave Motion* 16 (1992) 65–80.
[16] P.P. Delsanto, R.S. Schechter, H.H. Chaskelis, R.B. Mignogna, R. Kline, Connection machine simulation of ultrasonic wave propagation in materials. II: the two-dimensional case, *Wave Motion* 20 (1994) 295–314.
[17] S. Sundararaman, D.E. Adams, Modeling guided waves for damage identification in isotropic and orthotropic plates using a local interaction simulation approach, *Journal of Vibration and Acoustics, Transactions of the ASME*, 130, 2008, Article number 041009.
[18] J. Virieux, SH-wave propagation in heterogeneous media: velocity–stress finite-difference method, *Geophysics* 49 (1984) 1933–1942.
[19] J. Virieux, P-SV wave propagation in heterogeneous media: velocity–stress finite-difference method, *Geophysics* 51 (1986) 889–901.
[20] J.C. Strickwerda, *Finite Difference Schemes and Partial Differential Equations*, Wadsworth-Brooks, Belmont, 1989.
[21] I. Harari, E. Turkel, Accurate finite difference methods for time-harmonic wave propagation, *Journal of Computational Physics* 119 (1995) 252–270.
[22] D.W. Zingg, Comparison of high-accuracy finite-difference methods for linear wave propagation, *SIAM Journal of Scientific Computing* 22 (2001) 476–502.
[23] O. Gosselin, J.L. Teron, L. Nicoletis, Modeling of elastic wave propagation by finite-difference and finite-element methods, *Proceedings of IGARSS '84 Symposium, Strasbourg* Vol. 1 (1984) 549–552.
[24] G.S. Verdict, P.H. Glen, C.P. Burger, Finite element study of Lamb waves in a uni-directional graphite/epoxy plate, *American Society of Mechanical Engineers, Petroleum Division* 45 (1992) 31–38.
[25] M. Koshiba, S. Karakida, M. Suzuki, Finite-element analysis of Lamb wave scattering in an elastic plate waveguide, *IEEE Transactions on Sonics and Ultrasonics* 31 (1984) 18–25.
[26] F. Moser, L.J. Jacobs, J. Qu, Modeling elastic wave propagation in waveguides with the finite element method, *NDT and E International* 32 (1999) 225–234.
[27] T. Yokoyama, Finite element computation of torsional plastic waves in a thin-walled tube, *Archive of Applied Mechanics* 71 (2001) 359–370.
[28] M.J. Conry, L.J. Crane, M.D. Gilchrist, Ultrasonic detection of embedded and surface defects in thin plates using Lamb waves, *Proceedings of SPIE—The International Society for Optical Engineering* 4763 (2002) 180–186.
[29] S.M. Jeong, M. Ruzzene, Analysis of vibration and wave propagation in cylindrical grid-like structures, *American Society of Mechanical Engineers Dynamic Systems and Control Division* 72 (2003) 41–50.

[30] J. Zhu, A.H. Shah, S.K. Datta, BEM for scattering of elastic waves by cracks in laminated plates, *Proceedings of Engineering Mechanics* 1 (1995) 66–69.
[31] Y. Clio, Estimation of ultrasonic guided wave mode conversion in a plate with thickness variation, *IEEE Transactions on Ultrasonics, Ferroelectrics, and Frequency Control* 47 (2000) 591–603.
[32] T. Hayashi, S. Endoh, Calculation and visualization of Lamb wave motion, *Ultrasonics* 38 (2000) 770–773.
[33] C. Lu, L.X. Li, Z.K. Tu, D.Q. Zou, Boundary element analysis and experiments of propagation characteristics of ultrasonic subsurface longitudinal waves in railheads, *Journal of the China Railway Society* 30 (2008) 65–70.
[34] A.T. Patera, A spectral element method for fluid dynamics: laminar flow in a channel expansion, *Journal of Computational Physics* 54 (1984) 468–488.
[35] W. Dauksher, A.F. Emery, Accuracy in modeling the acoustic wave equation with Chebyshev spectral finite elements, *Finite Elements in Analysis and Design* 26 (1997) 115–128.
[36] D. Komatitsch, J.P. Vilotte, R. Vai, J.M. Castillo-Covarrubias, F.J. Sańchez-Sesma, The spectral element method for elastic wave equations—application to 2-D and 3-D seismic problems, *International Journal for Numerical Methods in Engineering* 45 (1999) 1139–1164.
[37] A. Żak, M. Krawczuk, W. Ostachowicz, Propagation of in-plane waves in an isotropic panel with a crack, *Finite Elements in Analysis and Design* 42 (2006) 929–941.
[38] W. Ostachowicz, M. Krawczuk, A. Żak, P. Kudela, Damage detection in elements of structures by the elastic wave propagation method, *Computer Assisted Mechanics and Engineering Sciences* 13 (2006) 109–124.
[39] P. Kudela, W. Ostachowicz, Wave propagation modelling in composite plates, *Applied Mechanics and Materials* 9 (2008) 89–104.
[40] A. Baz, Spectral finite-element modeling of the longitudinal wave propagation in rods treated with active constrained layer damping, *Smart Materials and Structures* 9 (2000) 372–377.
[41] M. Palacz, M. Krawczuk, Analysis of longitudinal wave propagation in a cracked rod by the spectral element method, *Computers and Structures* 80 (2002) 1809–1816.
[42] S.P. Anderson, Higher-order rod approximations for the propagation of longitudinal stress waves in elastic bars, *Journal of Sound and Vibration* 290 (2006) 290–308.
[43] S.R. Bodner, J. Aboudi, Stress wave propagation in rods of elastic–viscoplastic material, *International Journal of Solids and Structures* 19 (1983) 305–314.
[44] W. Seemann, Transmission and reflection coefficients for longitudinal waves obtained by a combination of refined rod theory and FEM, *Journal of Sound and Vibration* 198 (1996) 571–587.
[45] J. Zheng, P. Xu, Q. Fu, R.P. Taleyarkhan, S.H. Kim, Elastic stress waves of cylindrical rods subjected to rapid energy deposition, *Proceedings of the Institution of Mechanical Engineers, Part C: Journal of Mechanical Engineering Science* 218 (2004) 359–368.
[46] P. Kudela, M. Krawczuk, W. Ostachowicz, Wave propagation modelling in 1D structures using spectral finite elements, *Journal of Sound and Vibration* 300 (2007) 88–100.
[47] J.D. Achenbach, *Wave Propagation in Elastic Solids*, North-Holland Publishing Company, Amsterdam, 1973.
[48] J.L. Rose, *Ultrasonic Waves in Solid Media*, Cambridge University Press, Cambridge, 1999.
[49] L. Pochhammer, Biegung des Kreiscylinders–Fortpflanzungs-Geschwindigkeit kleiner Schwingungen in einem Kreiscylinder, *Journal für die Reine und Angewandte Mathematik* 81 (1876) 33–61.
[50] C. Chree, The equations of an isotropic elastic solid in polar and cylindrical coordinates, their solutions and applications, *Proceedings of the Cambridge Philosophical Society Mathematical and Physical Sciences* 14 (1889) 250–369.
[51] A.E. Love, *A Treatise on the Mathematical Theory of Elasticity*, fourth ed., Dover Publications, New York, 1927.
[52] R.M. Davis, A critical study of the Hopkinson pressure bar, *Philosophical Transactions of the Royal Society of London. Series A, Mathematical and Physical Sciences* 240 (1948) 375–457.
[53] Y.H. Pao, R.D. Mindlin, Dispersion of flexural waves in an elastic, circular cylinder, *Journal of Applied Mechanics* 27 (1960) 513–520.
[54] K.F. Graff, *Wave Motion in Elastic Solids*, Dover Publications, New York, 1991.
[55] URL: 〈http://www.mathworks.com〉.
[56] A. Ralston, *A First Course in Numerical Analysis*, McGraw-Hill Book Company, New York, 1965.
[57] T.R. Meeker, A.H. Meitzler, Guided wave propagation in elongated cylinders and plates, *Physical Acoustics*, Vol. 1, Part A, Academic Press, New York, 1964 (Chapter 2).
[58] A.H. Meitzler, Backward wave transmission of stress pulses in elastic cylinders and plates, *The Journal of Acoustical Society of America* 38 (1965) 835–842.
[59] A. Alippi, A. Bettucci, M. Germano, Anomalous propagation characteristics of evanescent waves, *Ultrasonics* 38 (2000) 817–820.
[60] P.L. Marston, Negative group velocity Lamb waves on plates and applications to the scattering of sound by shells, *The Journal of the Acoustical Society of America* 113 (2003) 2659–2662.
[61] R.D. Mindlin, G. Herrmann, A one-dimensional theory of compressional waves in an elastic rod, *Proceedings of the First U.S. National Congress of Applied Mechanics-1951*, 1952, pp. 187–191.
[62] URL: 〈http://www.wolfram.com/〉.